



HAL
open science

An improved hydrodynamic model for percolation and drainage dynamics for household and agricultural waste beds

Laura Digan, Pierre Horgue, Gerald Debenest, Simon Dubos, Sébastien Pommier, Etienne Paul, Claire Dumas

► **To cite this version:**

Laura Digan, Pierre Horgue, Gerald Debenest, Simon Dubos, Sébastien Pommier, et al.. An improved hydrodynamic model for percolation and drainage dynamics for household and agricultural waste beds. Waste Management, 2019, 98, pp.69-80. 10.1016/j.wasman.2019.07.027 . hal-02538675

HAL Id: hal-02538675

<https://hal.science/hal-02538675v1>

Submitted on 9 Apr 2020

HAL is a multi-disciplinary open access archive for the deposit and dissemination of scientific research documents, whether they are published or not. The documents may come from teaching and research institutions in France or abroad, or from public or private research centers.

L'archive ouverte pluridisciplinaire **HAL**, est destinée au dépôt et à la diffusion de documents scientifiques de niveau recherche, publiés ou non, émanant des établissements d'enseignement et de recherche français ou étrangers, des laboratoires publics ou privés.



Open Archive Toulouse Archive Ouverte



OATAO is an open access repository that collects the work of Toulouse researchers and makes it freely available over the web where possible

This is an author's version published in: <http://oatao.univ-toulouse.fr/25717>

Official URL:

<https://doi.org/10.1016/j.wasman.2019.07.027>

To cite this version:

Digan, Laura and Horgue, Pierre  and Debenest, Gérald  and Dubos, Simon and Pommier, Sébastien and Paul, Etienne and Dumas, Claire *An improved hydrodynamic model for percolation and drainage dynamics for household and agricultural waste beds.* (2019) *Waste Management*, 98. 69-80. ISSN 0956-053X .

Any correspondence concerning this service should be sent to the repository administrator: tech-oatao@listes-diff.inp-toulouse.fr

An improved hydrodynamic model for percolation and drainage dynamics for household and agricultural waste beds

Laura Digan^a, Pierre Horgue^b, Gérald Debenest^b, Simon Dubos^a, Sébastien Pommier^a, Etienne Paul^a, Claire Dumas^{a,*}

^aTBI, Université de Toulouse, CNRS, INRA, INSA, Toulouse, France

^bINPT, UPS, IMFT (Institut de Mécanique des Fluides de Toulouse), Université de Toulouse, Allée Camille Soula, F-31400 Toulouse, France and CNRS, IMFT, F-31400 Toulouse, France

A B S T R A C T

This study focuses on the hydrodynamic modelling of percolation and drainage cycles in the context of solid state anaerobic digestion and fermentation (VFA platform) of household solid wastes (HSW) in leach bed reactors. Attention was given to the characterization of the water distribution and hydrodynamic properties of the beds. The experimental procedure enabled the measurement of water content in waste beds at different states of compaction during injection and drainage, and this for two types of HSW and for two other type of wastes. A numerical model, set up with experimental data from water content measurements, highlighted that a capillary free dual porosity model was not able to correctly reproduce all the hydrodynamic features and particularly the drainage dynamics. The model was improved by adding a reservoir water fraction to macroporosity which allowed to correctly simulate dynamics. This model, validated with data obtained from agricultural wastes, enabled to explain more precisely the water behaviour during percolation processes and these results should be useful for driving either solid state anaerobic digestion or fermentation reactors. Indeed, this implies that the recirculation regime will impact the renewal of the immobile water fraction in macroporosity, inducing different concentration levels of fermentation products in the leachate.

Keywords:

Solid-state anaerobic processes
Leach-bed reactor
Dual-porosity model
Water transfer
Macroporous reservoir

1. Introduction

The continuous growth of the world population is expected to generate an increasing amount of waste. In 2012, the production of global municipal solid wastes generation reached around 1.3 Gt/year and this figure may double by 2025 (Hoorweg and Bhada Tata 2012). Municipal solid wastes include a high organic fraction, especially coming from the residual household solid wastes.

Organic wastes are usually transformed into biogas for heat and power generation through anaerobic digestion but an alternative approach is carbon resource recovery. Indeed, anaerobic fermentation of organic wastes may be used to form Volatile Fatty Acids (VFAs) that are produced via the hydrolytic, acidogenic (and even acetogenic) phases of anaerobic digestion. The VFAs are interesting molecules either used for the production of chemicals (esters, carbonyl compounds, alcohols, alkanes) and biopolymers (polyhy

droxyalkanoates) known as the VFA platform, or used for the production bioenergy (Agler et al., 2011; Lee et al., 2014; Tamis et al., 2015; Cavallé et al., 2016).

Anaerobic digestion can be operated in two stage processes: two consecutive reactors are used to physically separate the hydrolytic/acidogenic and methanogenic phases (Vavilin et al., 2001). With methane as targeted product, the configuration of a Leach Bed Reactor (LBR) coupled to a methanogenic reactor has been applied at lab scale to treat different substrates with high organic dry matter content, including food wastes (Stabnikova et al., 2008; Xu et al., 2011), municipal solid wastes (Viéitez and Ghosh, 1999; Rodríguez Pimentel et al., 2015), agricultural wastes (Cysneiros et al., 2011; Jagadabhi et al., 2011). The LBR is a solid state fermentation process in which the solid substrate remains static while the leachate is recirculated through the bed. This concept was initiated by Chynoweth et al. (1992) whose objective was to develop a process overcoming usual limitations encountered with high solid substrates. Recirculation aims at maintaining a sufficient humidity in the bed, facilitating inoculation and mass diffusion between the solid and the flowing liquid (Jha et al., 2011; Francois et al., 2007; Lü et al., 2008; Stabnikova et al., 2008). The

* Corresponding author at: TBI, Université de Toulouse, CNRS, INRA, INSA, Toulouse, France.

E-mail address: claire.dumas@insa-toulouse.fr (C. Dumas).

main highlighted advantages of this technology are: (i) its simple design and thus its relatively low cost (Dogan et al., 2009; Cysneiros et al., 2012; Yap et al., 2016); (ii) the improvement of bacterial activity due to wetting (Pommier et al., 2007); (iii) the acceleration of the first degradation stages, particularly acidogenesis (Francois et al., 2007). In the perspective of producing VFAs, this technology has also the advantage to enable the simultaneous production and withdrawal of VFAs.

In the LBR, a fraction of water flows between solid particles (macro scale) while another fraction, which is not flowing, enables to humidify the solid phase (micro scale). VFAs are produced in contact of the substrate, in the micropores; they are then transferred to the macropores and can be recovered via the liquid flow (Veeken and Hamelers, 2000). The amount of flowing water determines the efficiency with which the VFAs can be transferred and taken out of the LBR (Shewani et al., 2017). Therefore, an adapted recirculation strategy needs to be implemented in order to better manage the residence time of VFAs in the LBR. An incomplete or misunderstanding of water mobility (water flow and retention ability, water transfer rates) and of solute exchanges may lead to an incomplete control of the process and therefore a reduced performance. Biological and chemical reactions are affected by water management within the process. Indeed, water can influence (i) the local concentration of products which potentially inhibit these reactions, (ii) the recovery of valuable intermediary products before their further transformation and (iii) the product concentrations which must be suitable for the targeted post process. Moreover, the choice of recirculation strategy (continuous or intermittent, appropriate flow rates and recirculation rates) depends on the hydrodynamic and physical properties of the waste beds. For instance, in several studies, authors investigated the effect of the amount of recirculated leachate (Chugh et al., 1998; Sponza and Ağdağ, 2004) as well as the effect of the injection mode of leachate (Benbelkacem et al., 2010; Clarke et al., 2016) on the degradation of MSW.

LBRs with high waste beds involve the compaction of the bottom layers. The physical transport properties (*i.e.* porosity, permeability, effective dispersion for instance) are significantly affected by a compaction process. This settlement, is called primary settlement or physical compressive settlement (Huet et al., 2012; Gourc et al., 2010). Such a process is related to the vertical load of the waste and to the water flow. At local scale, it leads to a decrease in porosity, air permeability and effective diffusion values (Kacem et al., 2009; Huet et al., 2012) and can therefore affect, for instance, the efficiency of water supply and/or mass transport processes.

Experimental protocols have been developed to determine the physical properties of a leach bed, which are implemented in models to predict water retention and transfer (Shewani et al., 2015). Dual porosity is usually applied in order to model the hydraulic behaviour of wastes leach beds (Stoltz et al., 2011; García Bernet et al., 2011; Shewani et al., 2015; Di Donato et al., 2003). The solid wastes bed is generally defined as a multiphase porous medium containing two fluid phases: a liquid phase and a gas phase (Stoltz et al., 2010). The porous structure is decomposed in two types of pores: (i) macropores are well connected large spaces in which the fluid phases flow, these spaces contain free/mobile/dynamic water; micropores are small spaces (into or between the solid particles) in which the fluid phases are static, they contain bound/immobile/static water. In micropores, water is mainly retained by capillarity (Stoltz et al., 2011) and saturation increases as a result of a water transfer mechanism, from macro to micropores. Indeed, micropores are able to collect water from the flow occurring in macro scale spaces (Tinet et al., 2011). The main reason why the wetting process must be rapid and efficient, is that the bacterial activity and the availability of nutrients and biodegradable substrate, are optimal when micropores are filled with water (Pommier et al., 2007) which increases reaction rates.

Dual porosity models are usually suggested in order to simplify the description of water flow in a porous medium and has been previously used for modelling water behaviour in waste (Tinet et al., 2011; Han et al., 2011). Such models are used because single domain models do not accurately describe the fluid flow, a parameter we here need to handle, which occurs in pores with characteristic sizes ranging from micrometres to centimetres. As previously suggested by Gerke and van Genuchten (1993) and Gårdenäs et al. (2006), the dual permeability model is one of the possible approaches to deal with such an issue. However, the model remains difficult to configure correctly since it requires exhaustive data such as relative permeability and retention curves (Gerke and van Genuchten, 1993). In a previous study, Shewani et al. (2015) tried to reproduce water behaviour in waste using a simplified dual porosity model without capillary pressure (fitting only the relative permeability curve). This work highlights the necessity to improve the model because the simplified approach did not allow to completely capture water dynamics. In their study, Larsson and Jarvis (1999) pointed out the difficulty of the model to correctly represent the drainage water concentrations in a structured clay soil for short term fluctuation cases. They assumed that tracers were stored in micropores and were not affected by the bypass flow occurring in macropores. Audebert et al. (2016) combined experiments and the test of different models in order to exhibit the importance of fracture flows in the case of leachate recirculation in wastes. In addition, the effects of compaction on physical properties are often ignored or implemented with strong simplifying assumptions in modelling. It is important to include the compaction process in experiments in order to link its effect to the physical properties and correctly use the numerical model. A simple experimental protocol was described by Shewani et al. (2015) for instance, to determine leach bed properties with and without compaction.

In the present study, the protocol and the dual porosity model proposed by Shewani et al. (2015) were adapted and improved in order to better capture the experimental results. Waste beds were evaluated in terms of physical structure, as well as water flow and transfer through the wastes materials. The characterisation was performed on different types of wastes, chosen to represent a wide range of substrates in terms of physical properties. The vertical constraint related to the waste layers stacking in higher beds was also considered. To overcome the lack of retention curves for macro and microporosities theoretically necessary to set up the model, a modified dual porosity model was proposed to correctly handle the drainage dynamics in leach bed using exclusively water content measurements. The model parameters were calculated from experimental data in order to compare the wastes, and to be able to predict wetting and drainage process to improve biological reactions. This physical and hydrodynamic characterisation is a key point for driving either solid state anaerobic digestion or fermentation reactors.

Even though this work focuses on laboratory scale LBRs, the methodology developed deals with unsaturated flows in porous media. It can then be applied to larger scale solid state processes involving percolation/trickling in porous beds such as dry batch anaerobic digesters and landfill cells. In these cases, the implementation of the model will be different due to the specificities related to the nature of the substrates, their mechanical properties, the organic loading rates, the time scales.

2. Experimental material and methods

2.1. Waste materials

Four different wastes were used in this study: real and artificial household wastes, cow manure and wheat straw. Real household solid waste (rHSW) was provided by a household wastes treatment

center located in Cavigny (Manche, France). The fermentation process in these wastes was already undergoing. It was sorted to remove the largest pieces, before being introduced into the percolation column. Artificial household solid wastes (aHSW) were made from commercial products in order to mimic real household solid wastes. The composition (see [Supplementary material, Table S1](#)) was established after a national household waste characterisation campaign ([ADEME et al., 2010](#)). Once completely reconstituted, the aHSW were stored at ambient temperature for one week before use, in order to simulate pre fermented wastes such as the received rHSW. Cow manure solid wastes (CM) were sampled from an experimental farm of the French National Polytechnic Institute located in the area of Toulouse (Midi Pyrénées, France). For percolation operations, no mechanical pre treatment was carried out. Wheat straw (WS) was received from the experimental farm near Toulouse (Midi Pyrénées, France) and was used in the percolation device without pre treatment. All wastes were stored at 4 °C before use, except from WS samples which were stored at ambient temperature away from heat and humidity.

2.2. Chemical characteristics of the wastes

The wastes were chemically characterised in terms of total solids (TS) and volatile solids (VS). To measure the initial gravimetric water content of the raw matter, and thus TS content, a fresh sample of each waste was dried. For rHSW and aHSW samples, the drying was performed at 80 °C until obtaining a constant mass, in order to prevent any loss of the waste's organic fraction by combustion ([Stoltz et al., 2011](#)). CM and WS samples were dried at 105 °C for 24 h. The VS content was determined for all wastes by burning the previously dried samples at 550 °C for 2 h.

The chosen wastes covered a wide range of initial humidity contents, from the driest (WS, 94% TS) to the wettest (CM, 42% TS), rHSW and aHSW contained 49 and 69% of TS. VS accounted for 53% and 63% of TS for rHSW and aHSW, 80 and 92% of TS for CM and WS, showing a high organic matter content which justifies their suitability for fermentation. For more information on chemical characteristics of the wastes, the reader should refer to [Supplementary material, Table S2](#).

2.3. Experimental set up

The experimental device deployed for the hydraulic tests (see [Supplementary material, Fig. S1](#)) was similar to the one used by [Shewani et al. \(2015\)](#) and composed of a steel column with a diameter of 0.40 m and a height of 0.75 m. A grid placed at the bottom of the column prevented large solid particles from flowing out and clogging the exit nozzles. The waste beds were built with a height of about the diameter of the column (36 cm for HSW and around 40 cm for CM and WS). The wastes were added gradually in layers of approximately 10 cm while avoiding to press the solid wastes; thus, the bed was uniform across its whole height. A drainage layer composed of gravel (size of 6–14 mm) was added under the rHSW and aHSW beds to facilitate the leachate flow and avoid clogging by particles. The gravel layer had a height of 0.04 m, representing 10% of the total bed height.

The waste beds had similar heights but due to variable water contents, they had a wide range of bulk densities: 189 and 539 kg m⁻³ for aHSW and rHSW, 313 kg m⁻³ for CM and WS bed had the lowest bulk density with 20 kg m⁻³ (see [Supplementary material, Table S2](#)).

The dry solids volume represented decreasingly 13.7, 7.8, 7.1, 1.2% m³ m⁻³ of total volume for respectively rHSW, CM, aHSW and WS (detailed calculation in [Section 2.5](#)). These values suggested a high total porosity fraction whatever the considered waste (more than 86%) (see [Supplementary material, Table S3](#)).

For feeding of the column, a tank of water was connected to a peristaltic pump (Masterflex 77800 50). Water could be injected either through the bottom of the column (immersion phase for pre wetting) directly from the pump to the central exit nozzle, or on top of the waste bed (percolation assays for hydrodynamic characterisation) using an injection system with 16 needles of 0.8 mm diameter distributed all over the column section (12 needles for CM leach bed). In all cases, the liquid was drained through the five exit nozzles and collected into a drainage tank placed under the column. The feeding and drainage tanks were weighed continuously and the weights of injected and drained water were recorded every 20 s.

2.4. Hydraulic test protocol

The protocol for the hydraulic characterisation of the waste beds was performed at ambient temperature. It consisted in 5 successive steps (see details [Supplementary material, Table S4](#)). At initial state, the waste bed was at compaction level 0 (CL 0). The first step was an “immersion and drainage” which allowed to initiate the wetting process and improve the percolation efficiency. It consisted of immersing the waste bed with water by a vertical upward flow to improve the release of air trapped within the matrix. The immersed bed was then left at rest and finally completely drained. A known mass was added on top of the waste bed during this step to avoid flotation effects. The added mass was not negligible for rHSW and aHSW (17.9 kg) so that the waste beds is considered to have reached compaction level 1 (CL 1). For CM and WS, the mass added was low (2.9 kg), thus the waste beds were very slightly compacted and the compaction level was CL 0*. The second step was a series of “percolation drainage” cycles. One cycle consisted of injecting water on top of the leach bed at a constant flow rate during 4–7 h and then stopping the injection to allow the water to drain for 17–20 h. The total duration of a cycle was 24 h. Percolation cycles were performed alternating high and low flow rates to obtain flow dependent water content measurements. Indeed, increasing the water flow in steady state induces an increase of the volume of water running off along the macroscale channels and therefore the dynamic water content. On the third step, a bed compaction was performed by applying a fixed mass above the waste beds for 24 h: the compaction level at this stage was then called CL 2 for all wastes. This operation mimicked an additional upper layer of waste exerting a pressure over the bed. On the fourth step, the compacted waste bed (CL 2) underwent a second “immersion and drainage” as described at step 1. The fifth and final step was a series of “percolation drainage” cycles identical to step 2.

The waste bed height was measured throughout the experiment. Settlement was supposed to be physical and not due to waste biodegradation. This assumption was made because: (i) no inoculum was introduced in the process and (ii) the total time of the experiment was relatively small compared to typical biodegradation times (one week). Thus, the dry solids mass was considered to remain constant ([Shewani et al. 2015](#); [Stoltz et al. 2011](#)).

2.5. Calculations

Several percolation drainage cycles were necessary to measure a stable amount of water fully retained in the micropores of the solid bed. Thus, knowing this volume of water, it was possible to identify the microporosity volume.

The masses of water injected in the solid bed and leachate recovered at the bottom of the column were continuously recorded and plotted versus time. The fraction of the injected water which was retained in the solid bed was deduced by difference. From these measurements, the micropores volume (V_m) was calculated

as the sum of initial water content with the injected volume which remained trapped. The dry solids volume (V_{DS}) was estimated as the ratio between the dry solids mass (calculated with the total solids content measured prior to the experiment) and the dry solids particle density (ρ_{SP}). ρ_{SP} (kgTS L^{-1}) was computed as proposed by Agnew and Leonard (2003):

$$\rho_{SP} = \left(\frac{VS}{1.55} + \frac{(1 - VS)}{2.65} \right)^{-1} \quad (1)$$

where VS is the volatile solids content expressed in kgVS kgTS^{-1} .

Finally, the macropores volume was deduced using the previously computed values V_{DS} and V_m .

The time evolution of water content during percolation and drainage cycles was then used to determine the hydrodynamic parameters: micropores saturation dynamics, macropores saturation and hydraulic conductivity and water exchange rates between porosities (see Sections 3.2 and 3.3).

3. Results and discussion

The experimental methodologies presented some differences (compaction levels, flowrates tested and rest times) for rHSW and aHSW on one hand, and for CM and WS on the other hand. Moreover, the waste beds had very diverse structures (see Section 2.3). The results mainly focus on the water behaviour in the case of HSW (real and artificial) with a brief comparison to agricultural solid wastes (CM and WS).

3.1. HSW leach beds structure

The waste beds underwent water additions and compaction which modified their structure (total porosity, macropores, and micropores). The three main fractions (dry solids, micropores and macropores volumes) were quantified using the protocol described in Section 2.4 at each step.

3.1.1. Wastes beds settlement and compressibility

The evolution of the waste beds volumetric fractions (decreasing between the beginning and the end of the experiment) is presented in Fig. 1.

A bed settlement occurred during the step 1 of the hydraulic characterisation protocol (initial immersion and drainage). The rapid drainage of leachate under the effect of gravity created a suction which drove the solid matrix towards the bottom (Shewani, 2016). We assume that this settlement was mainly due to the rearrangement (consolidation) of the bed when particles were transported during immersion and drainage. Another contribution to the consolidation may be due to the local increase of capillary forces which occurred in the humidified pores when the water content decreased (drainage phase).

Understanding and measuring the effects of the settlement process on physical properties is crucial. They alter the flow behaviour and this has been already studied (Stoltz et al., 2010). For HSW, the first settlement might be mostly due to the 18 kg weights added on top of the beds to avoid flotation during step 1. From state CL 0 to CL 1, the bed porosity decreased from 86.3% to 81.1% for rHSW and from 92.9% to 88.9% for aHSW. No further settlement was observed over the first percolation series. At CL 2 stage, the total bed porosity (micro and macroporosity) accounted for 79.5% and 87.6% of total bed volume for rHSW and aHSW respectively. The compaction slightly amplified bed subsidence (step 4). For both HSWs, the bed volume did not decrease over the second percolation series. The total lost volume represented 33% and 43% of the initial bed volume for rHSW and aHSW respectively.

It is assumed that compressibility is characterised by the relative volume loss due, on one hand to physical compression, and on the other hand to water drainage. The smaller the initial dry solids volume fraction (or the higher the initial void volume fraction), the greater the total volume loss. Compressibility was thus a waste dependent parameter. Indeed, this parameter is driven by the waste composition (i.e. organic and mineral matter contents) (Chen et al., 2009), the elements size and their arrangement inside the matrix. At an industrial scale, the bottom layer of the waste bed is liable to be compacted due to the above staking layers, and this could foster the reduction of leachate flow.

3.1.2. Evolution of waste bed porosity under compaction

The total porosity was globally high (from 79.4 to 86.3% for rHSW and from 87.6% to 92.9% for aHSW) at every stage of the experiment. After the first compaction (CL 1), the microporosity

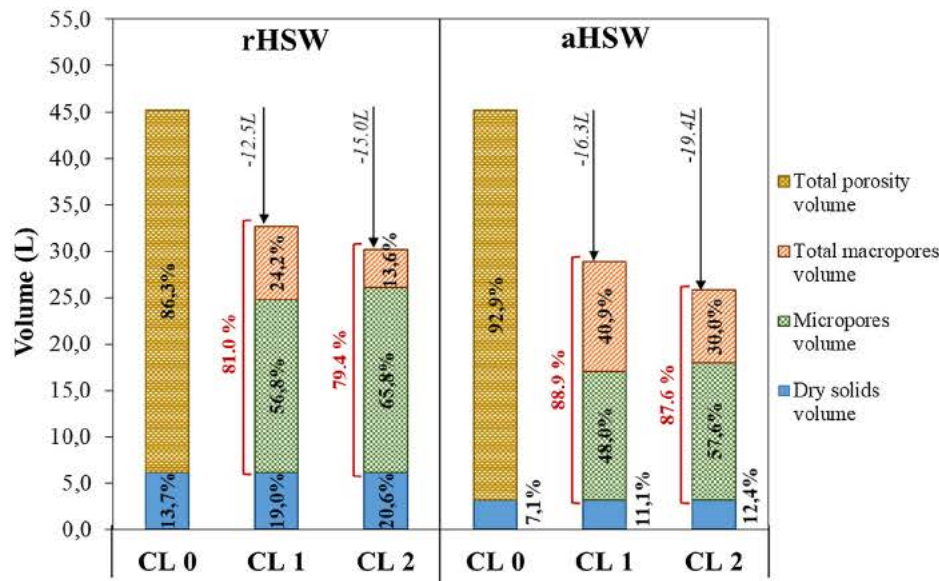


Fig. 1. Distribution of the different volumetric fractions in the waste beds at initial state (CL0), after the first (CL1) and second (CL2) percolation–drainage series. The values in percentage are the volume fractions of each element (ratio of volume of the element and volume of the bed).

of the beds reached 56.8% and 48.0% of the total volume for rHSW and aHSW respectively. At compaction level CL 2, microporosity fraction increased, representing 65.7% and 57.8% of total bed volume for rHSW and aHSW respectively. The increase of microporosity is made on the detriment of the macroporosity fraction. Indeed, macroporosity reduced from 24.2% at CL 1 to 13.6% at CL 2 for rHSW, and from 40.9 to 30.0% for aHSW, which suggests that the waste bed was rearranged. The macropores volume was partially converted into a microporous volume, which affected the hydrodynamic properties of the medium (See [Supplementary material, Table S5](#)). These results are consistent with those obtained by [Stoltz et al. \(2011\)](#) who studied the evolution of pore size distribution with compression. Authors observed that mechanical compression of the solid material induced an increase of smaller pores and a decrease of larger pores. Since the fluid phases flow through the macropores, the reduction of macroporous volume may affect the water flow through the material ([Reddy et al., 2009](#)). Moreover, a gain in microporosity may increase the water retention capacity and could foster efficient contact (due to larger surfaces) between the substrate and the bacterial populations.

3.2. Leach bed behaviour towards water

3.2.1. Waste imbibition, micropores saturation

Considering the injected mass of water injected in the leach bed and of recovered leachate, it was possible to calculate the amount of retained water initially injected in the waste leach bed. [Fig. 2](#) shows a typical evolution of the total water content over a cumulated contact time. We define the contact time as the time, whatever the step of the protocol considered, when 90% of the total drained volume was collected. This occurred after injection, rest and drainage for immersion drainage steps, and after injection and drainage for each percolation drainage cycle. The cumulated contact time was thus the sum of each contact time (for a series of experiments).

Successive injection and drainage phases led to a progressive increase of total amount of retained water within the bed, due to the imbibition of the waste. Considering the evolution of the total water content over time, the dynamic and static water contributions were dissociated using the values of water trapped in the

solid waste bed after each percolation drainage cycle. This enabled to evaluate the imbibition dynamics of the waste (static water curve in [Fig. 2](#)). Numerical simulations were then undertaken to determine the filling rate of the microporosity α_{micro} (see [Section 3.3.2](#)).

The evolution of microsaturation was plotted against total cumulated contact time, before and after the compaction step ([Fig. 3](#)). During the compaction step, a small volume of water, trapped in the microporosity, flowed out of the waste beds due to the applied overhead pressure. At the same time, the microporosity volume increased (see [Section 3.1.2](#)) and therefore, micropores saturation reduced from 100% to 89% for all waste beds (initial points of the graph B in [Fig. 3](#)). On the other hand, the filling behaviours before and after compaction were similar.

The results obtained in this study showed that the time needed to reach 80% microsaturation was approximately 3 days which is relatively short compared to the characteristic time of anaerobic digestion process which generally runs over more than 20 days. However, acidogenic fermentation processes are operated for a few days only and the transient wetting period of 3 days could reduce the overall performance.

3.2.2. Hydraulic conductivity, mobile water analysis

Hydraulic conductivity reflects the ability of a fluid to flow through a multiphase material ([Richard et al. 2004](#)) and represents the maximum fluid velocity for gravity driven flows. As described in previous studies investigating percolation regimes, flow rates are below the saturated hydraulic conductivity which leads to in unsaturated flows ([Shewani et al. 2015](#); [Gens Solé et al. 2011](#)). The characterisation of the relationship between the applied flow rate and the level of saturation (*i.e.* the volume of flowing water) is necessary to correctly predict water transfer between macro and microporosity as well as any other transfer (such as VFA transfer, not characterised here but see [Shewani et al. \(2017\)](#)). A good knowledge of water and flow distribution is then useful to adapt the leachate management strategy to the objective of the process (washing VFAs or increasing the concentration).

The apparent hydraulic conductivity (m s^{-1}) K_L used in the numerical model is defined as the product of the intrinsic

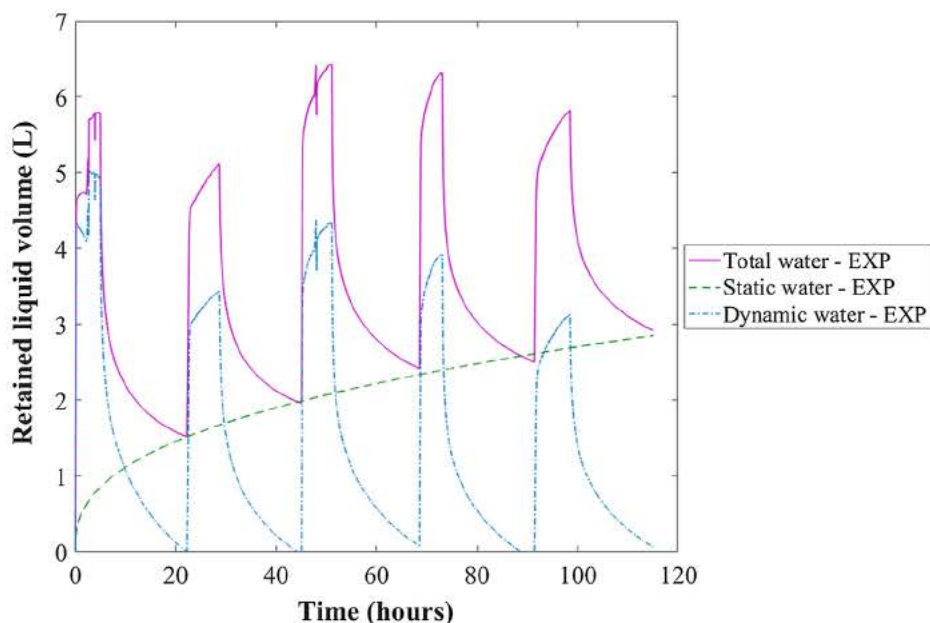


Fig. 2. Typical evolution of total water content over a percolation-drainage series. Total water is decomposed in static water and dynamic water.

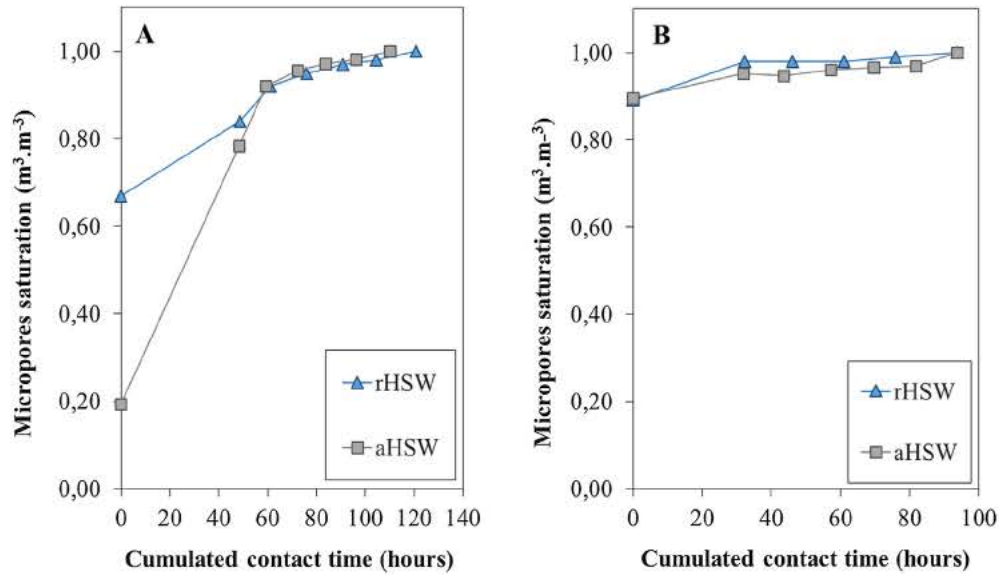


Fig. 3. Evolution of microsaturation as a function of the cumulated contact time during percolation series for the CL 1 (A) and CL 2 (B) configurations.

(or saturated) hydraulic conductivity (k_M) and relative hydraulic conductivity (or permeability) ($k_{r,L}$):

$$K_L = \underbrace{k_M}_{\text{intrinsic conductivity}} \cdot \underbrace{k_{r,L}}_{\text{relative conductivity}} \quad (2)$$

While k_M is an intrinsic function of medium parameters (porosity, tortuosity, pore size distribution and shape), $k_{r,L}$ is a function of medium parameters and dynamic variables such as macropores saturation (Wu, 2016). The apparent conductivity K_L was directly deduced from the experimental flow rate applied and plotted as a function of macropores saturation S_{Macro} (estimated by measuring the retained dynamic water) in Fig. 4.

For both cases CL 1 and CL 2, the aHSW bed showed lower macropores saturations compared to rHSW which means that the conductivity of aHSW was higher and would be able to accept larger flow rates, without flowing on the reactor sides. This was particularly true in the case of rHSW CL 2 (Fig. 4B) where pores were

almost saturated for the highest flow rate (macropores saturation >0.8) while it remained relatively unsaturated for aHSW (macropores saturation >0.4). The fact that the aHSW bed could accept higher flow rates, is possibly due to a more homogeneous structure related to the reconstitution of an artificial HSW. In a real case, as for rHSW, the wastes bed is heterogeneous, composed of various sizes of elements which may therefore show a lower apparent hydraulic conductivity.

3.3. Modelling water behaviour in wastes leach beds

Experiments allowed to observe water behaviour during percolation and drainage in waste beds. A model was implemented with the aim to describe more precisely the experimental observations, to predict water retention and transfer, and to correctly reproduce wetting and drainage processes. This can help in predicting the coupling of water transport phenomena with the biological reactions present during the fermentation/anaerobic digestion process.

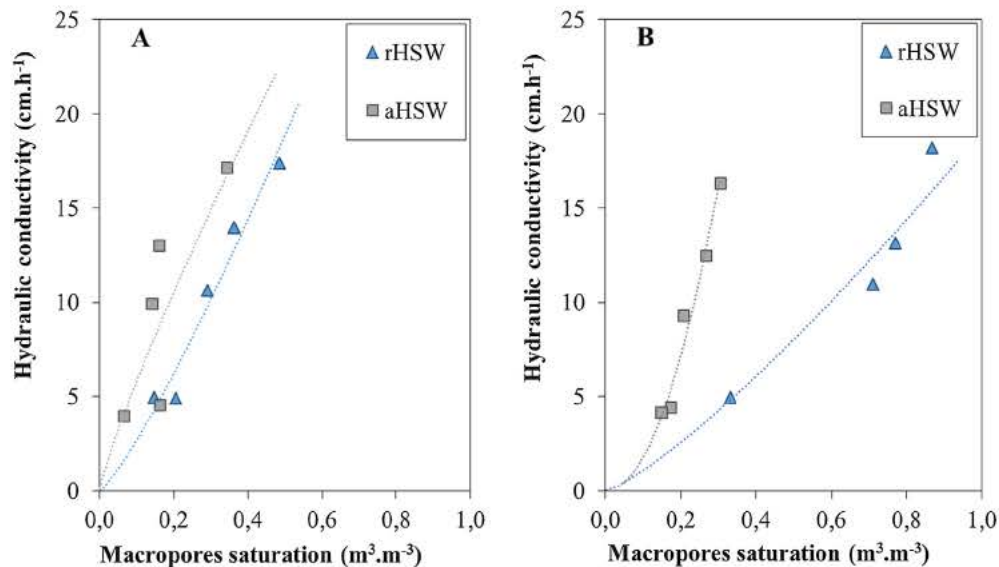


Fig. 4. Hydraulic conductivity K_L represented as a function of macropores saturation during percolation series for CL1 (A) and CL2 (B) configurations.

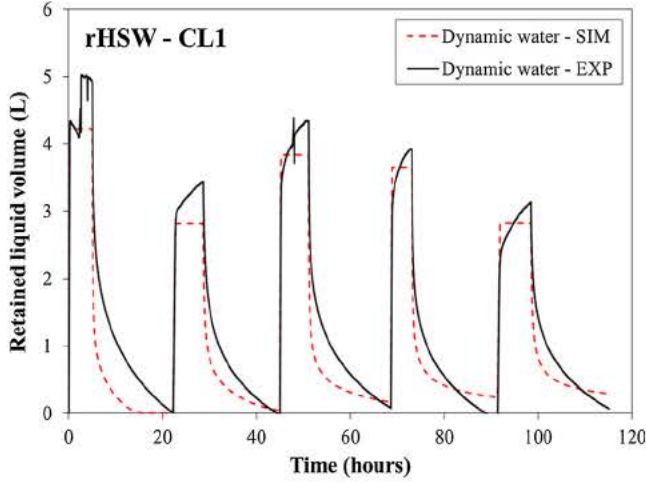


Fig. 5. An example of dynamic water modelling with classical porous medium model.

3.3.1. Limitation of simplified dual porosity model applied to household solid wastes

In a previous study (Shewani et al., 2015), a simplified capillary free dual porosity model was used to simulate water evolution in solid waste beds during several series of percolation drainage cycles.

In the present study, the simplified dual porosity model was applied to real and artificial household wastes (rHSW, aHSW). The comparison between experimental and numerical simulation of dynamic water curves showed that, whichever the type of waste and compaction level, the water dynamics were not completely reproduced (see Fig. 5). This was notably true for the drainage phase, as observed by Shewani et al. (2015) when studying cattle manure and wheat straw substrates. Indeed, the drainage dynamics depend both on relative permeability and water retention curves of the two porosities which are not handled in the simplified dual porosity model. The drainage dynamics, which were numerically too fast compared to the experimental observations, cannot be calibrated independently using only relative permeability curves. Moreover, the observation of the experimental drainage curves showed that the drainage dynamics were similar independently of the applied flow rate. The similarity between the curves suggested that only the "slow drainage part" is independent from the applied flow rate.

3.3.2. Implementing reservoir water to the mathematical model: description of the proposed model

In this work, the dual porosity model was improved to obtain a more realistic and predictive model of the drainage process. For that purpose, it was hypothesized that during the percolation process a part of the water located inside macroporosity is not actually flowing but temporarily immobile in the internal cavities of the waste and hereby called: reservoir water (see Graphical abstract). In the standard dual porosity model (Gerke and van Genuchten, 1993), when percolation occurs, the mobile water content increases, just as the head pressure, thereby inducing a water transfer from macro to microporosity (to equilibrate macro head pressure with the micro head pressure). When the injection is stopped, saturation in macroporosity as well as macro head pressure are reduced, which leads to a reverse water transfer from micro to macroporosity. The system reaches the equilibrium when gravity forces in macroporosity is balanced by capillary forces and when head pressure in both macro and microporosity are at the equilibrium. This equilibrium generally corresponds to

a high level of saturation in microporosity and a low level of saturation in macroporosity, since capillary effects are higher in micropores. In the proposed model, an additional parameter is introduced to divide the microporosity into two porosities: (i) the static water which remains trapped even after drainage and (ii) the reservoir water which is trapped temporarily when mobile water is flowing through. Since this reservoir water is recovered during the drainage, we considered in our model that it belongs to macroporosity. This dissociation is made possible by considering that the filling and drainage time of the mobile water are negligible compared to that of the reservoir water.

The 3 conservation equations numerically related to saturation (S) are:

$$\underbrace{\epsilon_{Macro} \frac{\partial S_{Macro}}{\partial t}}_{\text{Mobile macroporosity saturation}} + \underbrace{\nabla \cdot U_{water}}_{\text{Mobile water transport}} \quad (3)$$

$$\underbrace{q_{Macro,res}}_{\text{Mobile - reservoir exchange}} + \underbrace{q_{micro}}_{\text{Mobile -static exchange}} + \underbrace{\epsilon_{Macro,res} \frac{\partial S_{Macro,res}}{\partial t}}_{\text{Macroporous reservoir saturation}} + \underbrace{q_{Macro,res}}_{\text{Mobile - reservoir exchange}} \quad (4)$$

$$\underbrace{\epsilon_{micro} \frac{\partial S_{micro}}{\partial t}}_{\text{Macroporous saturation}} + \underbrace{q_{micro}}_{\text{Mobile-static exchange}} \quad (5)$$

In these equations, ϵ_{Macro} , $\epsilon_{Macro,res}$ and ϵ_{micro} are the "mobile" macroporosity, the "reservoir" macroporosity and the microporosity volume fractions, respectively. S_{Macro} , $S_{Macro,res}$ and S_{micro} ($m^3 m^{-3}$) are the "mobile" macroporosity, the "reservoir" macroporosity and the microporosity saturations, respectively. $q_{Macro,res}$ ($m^3 m^{-3} s^{-1}$) is the term for the exchange between "mobile" and "reservoir" macroporous water. In the same way, q_{micro} ($m^3 m^{-3} s^{-1}$) is the term for the exchange between "mobile" macroporous water and static water.

A first order model is applied for the mobile reservoir exchange term $q_{Macro,res}$:

$$q_{Macro,res} = \begin{cases} \underbrace{\alpha_{res,charge}}_{\text{Exchange coefficient for reservoir charge}} \begin{pmatrix} 1 \\ \underbrace{S_{Macro,res}}_{\text{Macroporous reservoir saturation}} \end{pmatrix} & \text{if charge} \\ \underbrace{\alpha_{res,discharge}}_{\text{Exchange coefficient for reservoir discharge}} \begin{pmatrix} \underbrace{S_{Macro,res}}_{\text{Macroporous reservoir saturation}} \end{pmatrix} & \text{if discharge} \end{cases} \quad (6)$$

And for the mobile static exchange term q_{micro} (exclusively in charge since water remains trapped in microporosity):

$$q_{micro} = \underbrace{\alpha_{micro}}_{\text{Exchange coefficient for micropores charge}} \begin{pmatrix} 1 \\ \underbrace{S_{micro}}_{\text{Micropores saturation}} \end{pmatrix} \quad (7)$$

$\alpha_{res,charge}$ and $\alpha_{res,discharge}$ (s^{-1}) respectively stand for the exchange coefficient between “mobile” and “reservoir” macroporous water during the charge and discharge cycles. α_{micro} (s^{-1}) is the exchange coefficient between “mobile” macroporous water and static water.

The water mobile velocity U_{water} ($m s^{-1}$) is modelled and computed using the generalized Darcy’s law with a classical Brooks and Corey (power law) model for relative permeability (Brooks and Corey, 1964):

$$\underbrace{U_{water}}_{\text{Mobile water velocity}} \cdot \underbrace{K_L}_{\text{Hydraulic conductivity}} \cdot \underbrace{S_{Macro}^p}_{\text{Mobile macroporosity saturation}} \quad (8)$$

where K_L ($m s^{-1}$) is the hydraulic conductivity of the porous medium, and p is the Brooks and Corey coefficient. The Brooks and Corey parameters K_L and p are evaluated in order to fit experimental points available. This allows the evaluation of the mobile water content (macrosaturation) for a given flow rate during numerical simulations (dash lines in Fig. 4). The Brooks and Corey model is one of the main models used for permeability (and therefore hydraulic

conductivity) correlations. Stoltz et al. (2011) also calibrated this type of model with real municipal solid wastes for drainage retention properties and concluded that it was applicable to these types of wastes.

For a given waste composition, all the parameters need to be characterised by experimental measurements: the 3 porosities (ϵ_{Macro} , $\epsilon_{Macro,res}$ and ϵ_{micro}), the 3 exchange rates ($\alpha_{res,charge}$, $\alpha_{res,discharge}$ and α_{micro}) and the coefficients (K_L and p) for the relative permeability law. An 8 parameter optimization is complex to set up and would require excessive computation times. Moreover, characteristic times between processes are different (imbibition of the waste is much slower than filling/emptying the reservoir part and the mobile saturation variations are fast and considered as instantaneous) which allows a progressive parametrisation as described in Section 3.3.3.

3.3.3. Application of improved dual porosity model to HSW

In this part, it is considered that static/dynamic water decomposition has been delineated in independent experiments described in Section 3.2.1 (ϵ_{micro} and α_{micro} are already characterised). Therefore only the evolution of dynamic water (which cannot be reproduced by a simplified model) is studied.

In order to determine the “reservoir” macroporosity fraction, experimental drainage curves were time shifted and plotted to position the initial time at the point where injection was stopped (see an example for rHSW sample in Fig. 6). In these conditions, the drainage curves were similar for all tested flow rates, i.e. starting with a quasi instantaneous drainage of a part of the water content followed by an inflection of the curve which indicated a slowdown of the drainage phase. The distinction between fast and slow drainage part is purely conceptual and cannot be determined precisely. From the experimental data, we determined the beginning of the slower drainage as the moment when the drainage flow rate measurement reached the experimental precision (0.01 L/min) which corresponded in our case to 10% of the maximal measured drainage flow rate. For the presented drainage curves (Fig. 6), the evaluated reservoir water content was equal to $2.28 L \pm 0.12$. The reservoir porosity $\epsilon_{Macro,res}$ was then directly computed from the evaluated reservoir water volume. ϵ_{Macro} was simply deduced from the previously determined microporous and

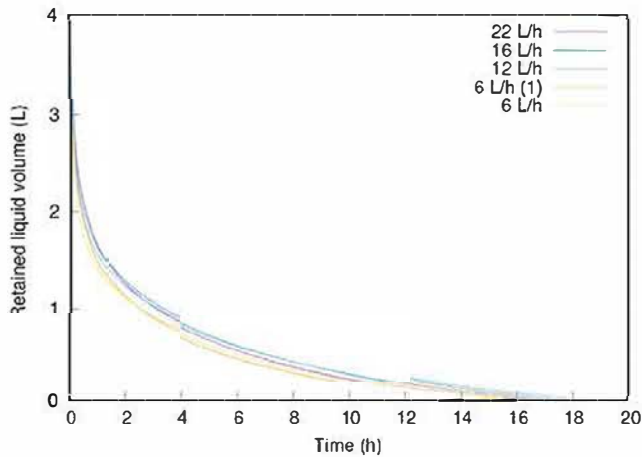


Fig. 6. Experimental drainage curves for rHSW-CL 1. Initial time corresponds to the moment when injection is stopped.

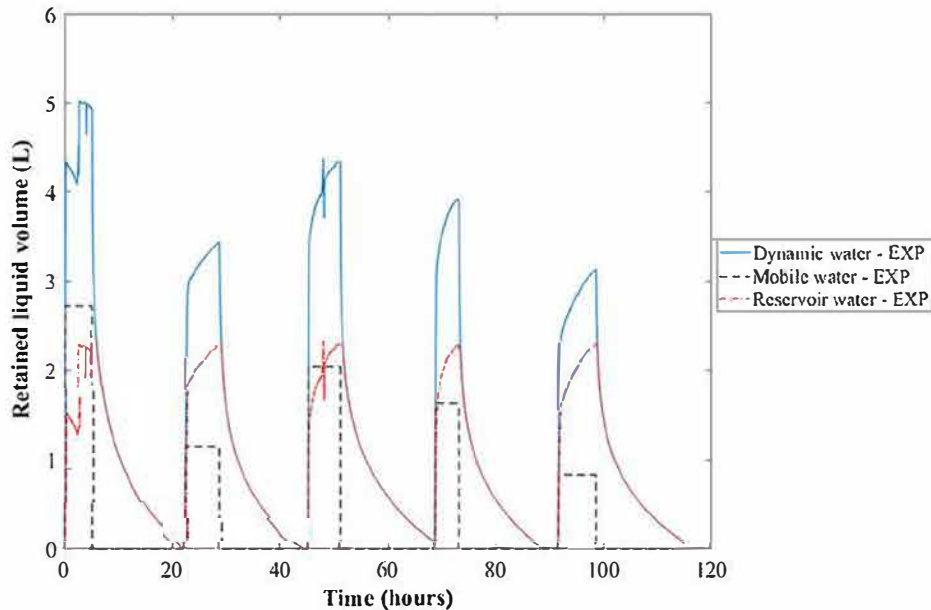


Fig. 7. Decomposition of dynamic water into mobile and reservoir waters. The decomposition is shown for the rHSW-CL1 case.

solid fractions. This hypothesis enabled the decomposition of dynamic water into mobile and reservoir macroporous water such as presented in Fig. 7.

From this decomposition, the Brooks and Corey parameters (K_L and p) could be directly fitted using the series of plateaus (as described in Section 3.2.2) while the charge $\alpha_{res,charge}$ and discharge $\alpha_{res,discharge}$ rate are calibrated using numerical simulations (see Table 1).

In Fig. 8, the evolution of dynamic water content over time from experiments and numerical simulations are presented for both rHSW and aHSW at two compaction levels (CL 1 and CL 2). Results showed a quite good representation of the percolation and drainage dynamics with the improved model, independently of the state of the beds and the type of waste. Fig. 9 shows an example of the relative prediction error in terms of water content using

the simplified and the improved “reservoir” dual porosity model. We observed that for all substrates tested, the “reservoir” approach enabled to maintain the prediction error close to or below 5% for the whole experiment except during very short moments, at the beginning of a percolation cycle for example. Using the simplified model, the error remained between 5% and 20% during most of the experiment, especially during drainage phases.

The general behaviour of both wastes are similar with the same charge rate of the reservoir macroporosity ($\alpha_{res,charge} = 1.29 \text{ day}^{-1}$). The discharge of reservoir macroporosity was a little bit slower for rHSW $\alpha_{res,discharge} = 0.26 \text{ day}^{-1}$ than for aHSW $\alpha_{res,discharge} = 0.35 \text{ day}^{-1}$. These observations were consistent with the higher hydraulic conductivity for aHSW than for rHSW (53.1 cm h^{-1} and 43.4 cm h^{-1} respectively).

Notably, the measured dynamic water content was higher in the second percolation cycle than in the last percolation cycle, although the flow rate was identical (low flow rate, 6L/h), and this for both wastes (Fig. 8). This highlights that partial wetting of the substrate has a significant influence on dynamic saturation during the first phase of imbibition.

Compaction seemed to have no influence on the charging rate of reservoir water, whatever the considered waste (rHSW or aHSW). However, compaction affected the discharge rate of reservoir water, with a decrease from 0.35 to 0.17 day^{-1} in the case of aHSW. Compaction involved a rearrangement of the bed structure which could explain the slower drainage of the reservoirs. However, this was not the case for rHSW beds.

Table 1
Parameters calculated with the proposed model for HSW.

	rHSW - CL1	rHSW - CL2	aHSW - CL1	aHSW - CL2
$\epsilon_{Macro,res}$	7,0%	6,0%	6,2%	3,9%
α_{macro} (day^{-1})	0.35	0.35	0.6	0.6
$\alpha_{res,charge}$ (day^{-1})	1.29	1.29	1.29	1.29
$\alpha_{res,discharge}$ (day^{-1})	0.26	0.26	0.35	0.17
K ($\text{cm}\cdot\text{h}^{-1}$)	43.4	19.0	53.1	184.0
p	1.21	1.24	0.89	2.02

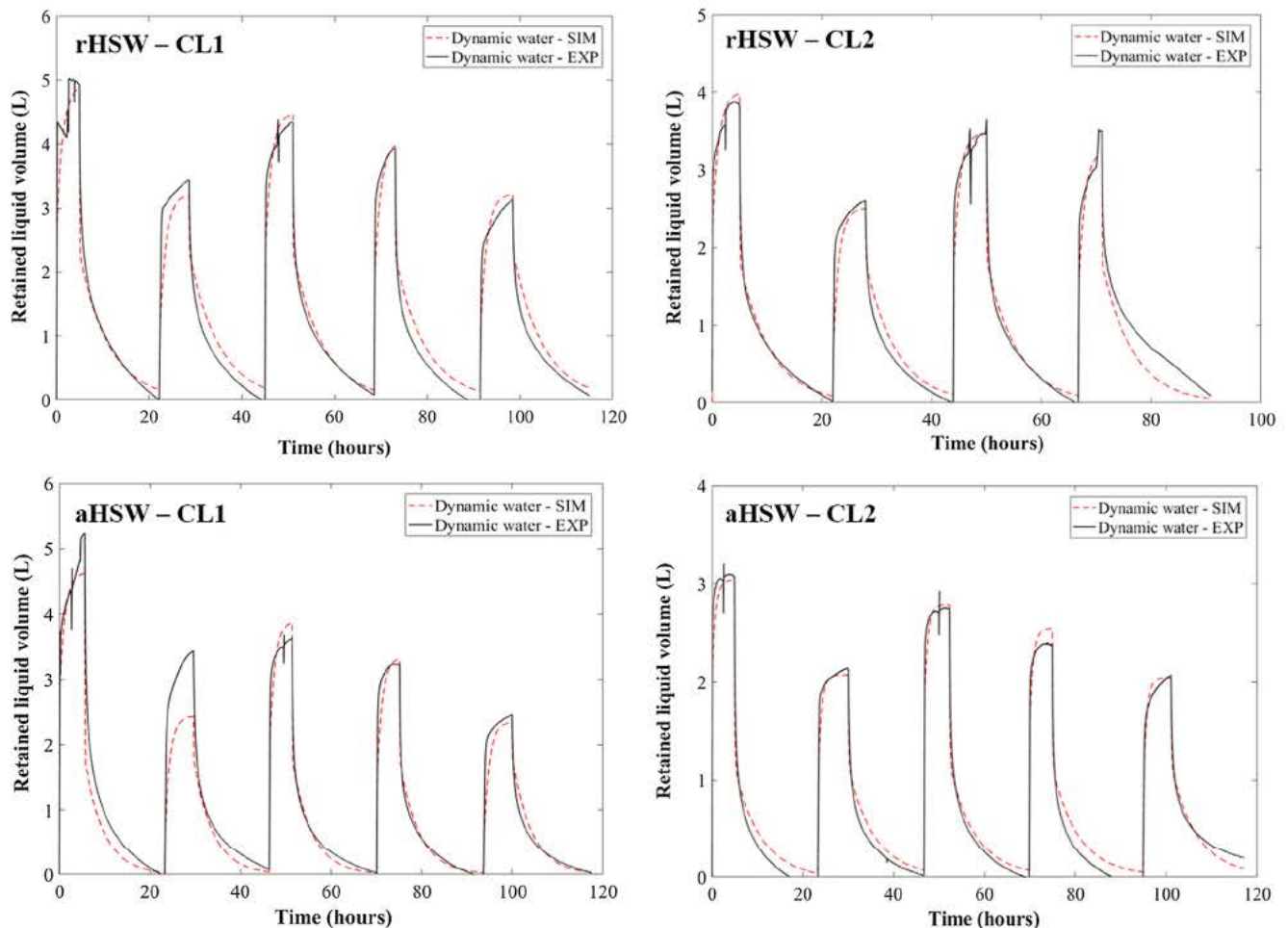


Fig. 8. Measured and simulated evolution of dynamic water content over time during percolation–drainage series for rHSW and aHSW. Dynamic water is plotted for all the different percolation flow rates.

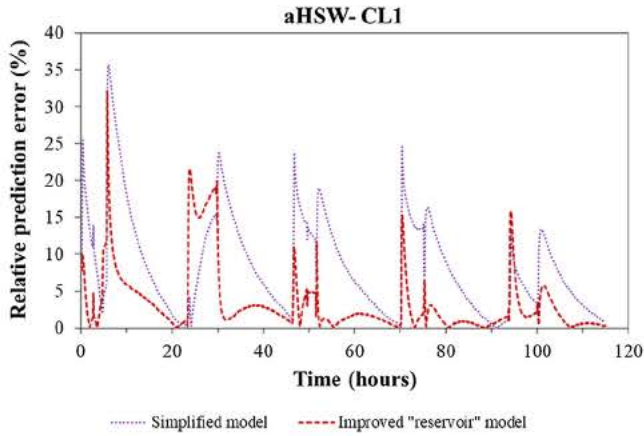


Fig. 9. Comparison of the simplified and improved models prediction errors for the aHSW-CL1 case.

3.3.4. Validation of the improved model on other types of wastes (CM and WS)

The model developed is a methodologic tool that aims at understanding the hydrodynamics in LBRs. The model was firstly developed on HSW, but in order to validate the method and show its applicability to a large variety of wastes, it was tested on two other waste beds: CM and WS, presented in Section 2.1. These wastes showed very different properties. In Fig. 10, the evolution of the

dynamic water content over time from experiments and numerical simulations are presented for CM and WS at two compaction levels (CL 0* and CL 2). It shows that the percolation and drainage dynamics are mostly well reproduced for all cases. This is particularly visible for the CM case which was studied in Shewani et al. (2015) and whose drainage dynamics is now properly captured.

The hydrodynamic parameters calculated with the numerical model are presented in Table 2.

As for static water retention, the exchange rate α_{micro} for CM was similar but slightly higher than for household waste beds at CL 0* and the same as rHSW at CL 2. For WS, the imbibition process is almost instantaneous ($\alpha_{micro} \rightarrow \infty$) independently of the compaction level. This can be explained by the elongated shape of wheat straw which offers a very large contact surface area between mobile and static water, coupled to the relative low microporosity of this substrate (almost halved).

Table 2
Parameters calculated with the proposed model for CM and WS.

	CM - CL0*	CM - CL2	WS - CL0*	WS - CL2
$\epsilon_{Macro, res}$	3.2%	4.0%	1.0%	2.0%
α_{micro} (day ⁻¹)	0.78	0.35	0	0
$\alpha_{res, charge}$ (day ⁻¹)	1.29	1.29	1.29	1.29
$\alpha_{res, discharge}$ (day ⁻¹)	0.26	0.13	0.17	0.17
K (cm·h ⁻¹)	6751.7	31.3	187.9	41.6
p	2.66	1.60	1	1

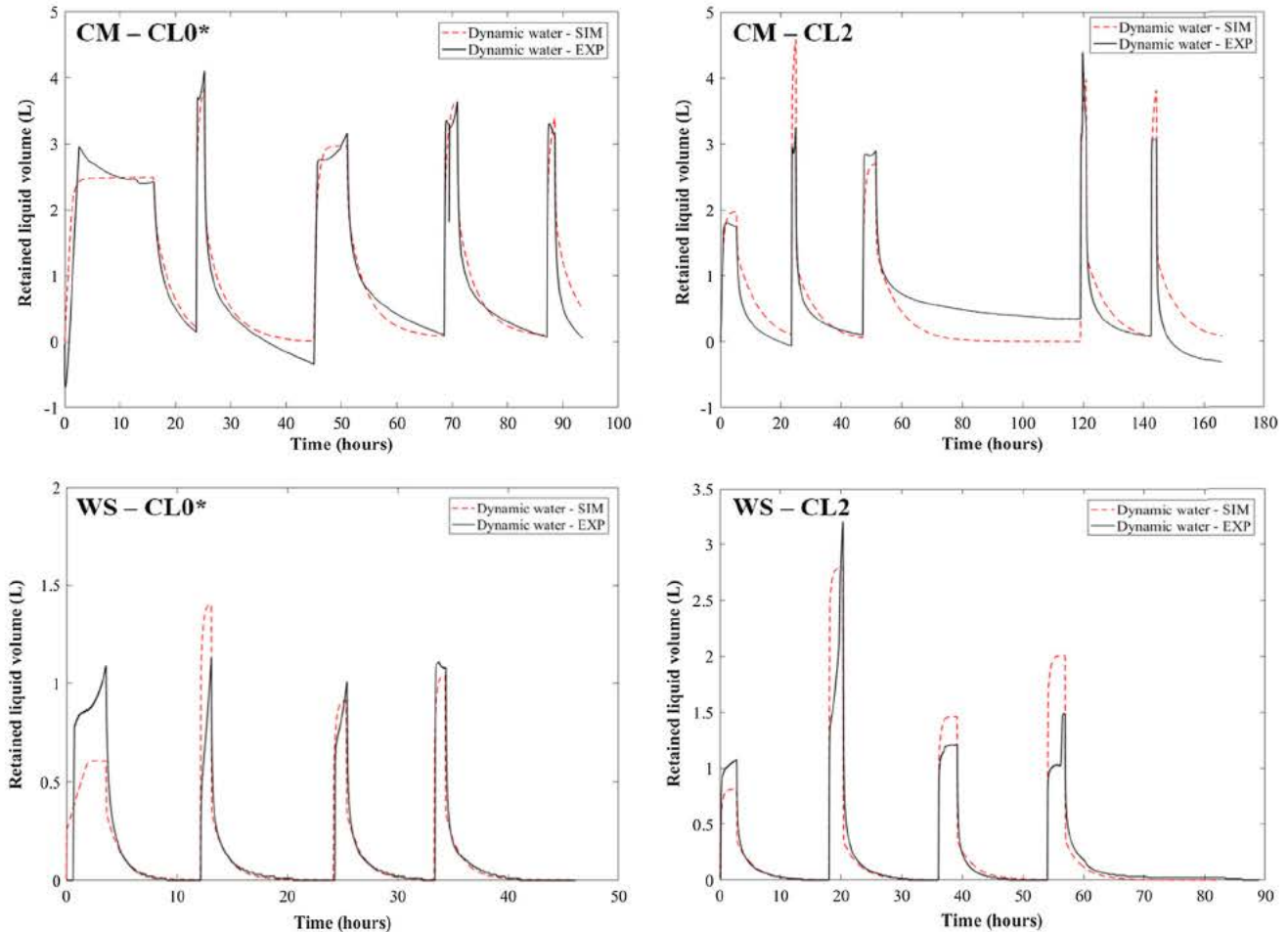


Fig. 10. Measured and simulated evolution of dynamic water content over time during percolation-drainage series for CM and WS. Dynamic water is plotted for all the different percolation flow rates.

Regarding the reservoir/mobile macroporous water exchange, the rates for reservoir macroporous water charge are at least five times higher than the discharge ones (as observed for HSW).

For CM, the evolution of the dynamic water content was similar to the household wastes with a discharge slightly slower after compaction ($\alpha_{res, discharge} = 0.26 \text{ day}^{-1}$ at CL 0* and $\alpha_{res, discharge} = 0.13 \text{ day}^{-1}$ at CL 2). This could be related to the smaller macroporous reservoir fraction in CM compared to rHSW and aHSW. For the WS substrate, charge and discharge rates were identical, and the value was the same as for the aHSW CL2 case. However, the estimated macroporous reservoir volume was very low, i.e. less than 2% of the total volume.

The model was applied to very different types of substrate beds. Even though dynamics were globally well reproduced, the limits of the model were highlighted for extreme cases, for instance the WS bed which was very dry and showed very rapid dynamics. Further studies could be performed on other types of substrates, such as different lignocellulosic materials. The experimental protocol will probably need to be readjusted to these specific substrates in order to correctly evaluate water retention dynamics.

3.4. Perspectives of application

The experimental procedure developed in the present study enabled to estimate physical parameters which allowed to calibrate the improved “reservoir” model on household solid wastes and to validate it on cow manure and wheat straw. The improved model could be incorporated into simulations of a real fermentation or anaerobic digestion process to determine optimum operating conditions. The water flow was described and explained with the presence of water in macroporous reservoirs. Indeed, the volume of these reservoirs and their charge and discharge rates may impact the products recovery.

An adapted recirculation strategy could be implemented in order to manage the residence time of VFAs within the LBR and could in turn influence, not only the VFAs spectrum, but also the local pH and hence inherent biological activities. Moreover, depending the downstream valuation targeted, the leachate management will not be the same. Continuous recirculation will not renew the macroporous reservoir water fraction, therefore the concentration in fermentation products might be low. Intermittent percolation will evacuate the immobile macroporous water fraction, and hence increase the concentrations of fermentation products in the leachate.

4. Conclusions

In this study, the various water dynamics occurring during percolation and drainage through solid waste leach beds were investigated for different types of wastes and under two compaction levels. The simplified capillary free dual porosity model was not able to completely reproduce the water dynamics, particularly in the drainage phase. Thus, the model has been extended by adding an immobile (reservoir) fraction to the macroporosity, which allowed to calibrate the model using only water content measurements without retention curves.

An improved experimental procedure was developed to correctly evaluate the effective parameters described in the model. The model enabled to correctly simulate dynamics for all configurations and to explain more precisely the behaviour of leachate and water during leaching processes. The new description of water flow highlighted the presence of water in macroporous reservoirs. Such results are important in the view of leachate recirculation strategy of waste digestion.

Acknowledgements

This work was supported by the project RECOVER funded by the Carnot Institute 3BCAR. The authors want to acknowledge French research ministry for Laura Digan PhD financial support. The authors would like to acknowledge also Anil Shewani, Zhe Li, Matthieu Peyre Lavigne, Mansour Bounouba, Evrard Mengelle, Simon Dubos, Chantha Kim, Michel Mauret and Xavier Lefebvre for their numerous contributions to the work. Authors also thank Monique Ras (Blue Science Consulting & Management: BSCM) for English revisions.

Appendix A. Supplementary material

Supplementary data to this article can be found online at <https://doi.org/10.1016/j.wasman.2019.07.027>.

References

- ADEME, Service public 2000, BRGM, CEMAGREF, 2010. *La composition des ordures ménagères et assimilées en France*. ADEME, Angers.
- Agler, M.T., Wrenn, B.A., Zinder, S.H., Angenent, L.T., 2011. Waste to bioproduct conversion with undefined mixed cultures: the carboxylate platform. *Trends Biotechnol.* 29 (2), 70–78. <https://doi.org/10.1016/j.tibtech.2010.11.006>.
- Agnew, J.M., Leonard, J.J., 2003. The physical properties of compost. *Compos. Sci. Utilizat.* 11 (3), 238–264.
- Audebert, M., Oxarango, L., Duquennoy, C., Touze-Foltz, N., Forquet, N., Clément, R., 2016. Understanding leachate flow in municipal solid waste landfills by combining time-lapse ERT and subsurface flow modelling – Part II: constraint methodology of hydrodynamic models. *Waste Manage., SI: Sanitary Landfilling* 55 (September), 176–190. <https://doi.org/10.1016/j.wasman.2016.04.005>.
- Benbelkacem, H., Bayard, R., Abdelhay, A., Zhang, Y., Gourdon, R., 2010. Effect of leachate injection modes on municipal solid waste degradation in anaerobic bioreactor. *Bioresour. Technol.* 101 (14), 5206–5212. <https://doi.org/10.1016/j.biortech.2010.02.049>.
- Brooks, R.H., Corey, A.T., 1964. *Hydraulic Properties of Porous Media Hydrology Papers*. Colorado State University.
- Cavaillé, L., Albuquerque, M., Grousseau, E., Lepeuple, A.-S., Uribelarra, J.-L., Hernandez-Raquet, G., Paul, E., 2016. Understanding of polyhydroxybutyrate production under carbon and phosphorus-limited growth conditions in non-axenic continuous culture. *Bioresour. Technol.* 201 (February), 65–73. <https://doi.org/10.1016/j.biortech.2015.11.003>.
- Chen, Y., Tony, M., Zhan, L.T., Wei, H.Y., Ke, H., 2009. Aging and compressibility of municipal solid wastes. *Waste Manage.* 29 (1), 86–95. <https://doi.org/10.1016/j.wasman.2008.02.024>.
- Chugh, S., Clarke, W., Pullammanappallil, P., Rudolph, V., 1998. Effect of recirculated leachate volume on MSW degradation. *Waste Manage. Res.* 16 (6), 564–573. <https://doi.org/10.1177/0734242X9801600607>.
- Chynoweth, D.P., Owens, J., O’Keefe, D., Earle, J.F.K., Bosch, G., Legrand, R., 1992. Sequential batch anaerobic composting of the organic fraction of municipal solid waste. *Water Sci. Technol.* 25 (7), 327–339. <https://doi.org/10.2166/wst.1992.0165>.
- Clarke, W.P., Xie, S., Patel, M., 2016. Rapid digestion of shredded MSW by sequentially flooding and draining small landfill cells. *Waste Manage., SI: Sanitary Landfilling* 55 (September), 12–21. <https://doi.org/10.1016/j.wasman.2015.11.050>.
- Cysneiros, D., Banks, C.J., Heaven, S., Karatzas, K.-A.G., 2011. The role of phase separation and feed cycle length in leach beds coupled to methanogenic reactors for digestion of a solid substrate (Part 2): hydrolysis, acidification and methanogenesis in a two-phase system. *Bioresour. Technol.* 102 (16), 7393–7400. <https://doi.org/10.1016/j.biortech.2011.05.042>.
- Cysneiros, D., Banks, C.J., Heaven, S., Karatzas, K.-A.G., 2012. The effect of PH control and “hydraulic flush” on hydrolysis and volatile fatty acids (VFA) production and profile in anaerobic leach bed reactors digesting a high solids content substrate. *Bioresour. Technol.* 123 (November), 263–271. <https://doi.org/10.1016/j.biortech.2012.06.060>.
- Di Donato, G., Huang, W., Blunt, M.J., 2003. Streamline-based dual porosity simulation of fractured reservoirs. *SPE Annual Technical Conference and Exhibition* <https://www.onepetro.org/conference-paper/SPE-84036-MS>.
- Dogan, E., Dunaev, T., Erguder, T.H., Demirer, G.N., 2009. Performance of leaching bed reactor converting the organic fraction of municipal solid waste to organic acids and alcohols. *Chemosphere* 74 (6), 797–803. <https://doi.org/10.1016/j.chemosphere.2008.10.028>.
- Francois, V., Feuillade, G., Matejka, G., Lagier, T., Skhiri, N., 2007. Leachate recirculation effects on waste degradation: study on columns. *Waste Manage.* 27 (9), 1259–1272. <https://doi.org/10.1016/j.wasman.2006.07.028>.
- García-Bernet, D., Buffière, P., Latrielle, E., Steyer, J.-P., Escudie, R., 2011. Water distribution in biowastes and digestates of dry anaerobic digestion technology. *Chem. Eng. J.* 172 (2–3), 924–928. <https://doi.org/10.1016/j.cej.2011.07.003>.

- Gårdenäs, Annemieke I., Šimůnek, Jirka, Jarvis, Nicholas, van Genuchten, M.Th., 2006. Two-dimensional modelling of preferential water flow and pesticide transport from a tile-drained field. *J. Hydrol.* 329 (3–4), 647–660. <https://doi.org/10.1016/j.jhydrol.2006.03.021>.
- Solé, Gens, Antonio, Beatriz Vállejan, Sánchez, M., Imbert, Christophe, Villar, Maria Victoria, Van Geetl, Maarten, 2011. Hydromechanical behaviour of a heterogeneous compacted soil: experimental observations and modelling. *Geotechnique* 61 (5), 367–386.
- Gerke, H.H., van Genuchten, M.T., 1993. A dual-porosity model for simulating the preferential movement of water and solutes in structured porous media. *Water Resour. Res.* 29 (2), 305–319. <https://doi.org/10.1029/92WR02339>.
- Gourc, J.-P., Staub, M.J., Conte, M., 2010. Decoupling MSW settlement into mechanical and biochemical processes – modelling and validation on large-scale setups. *Waste Manage.* 30 (8–9), 1556–1568. <https://doi.org/10.1016/j.wasman.2010.03.004>.
- Han, B., Scicchitano, V., Imhoff, P.T., 2011. Measuring fluid flow properties of waste and assessing alternative conceptual models of pore structure. *Waste Manage.* 31 (3), 445–456. <https://doi.org/10.1016/j.wasman.2010.09.021>.
- Hoornweg, D., Bhada-Tata, P., 2012. What a Waste : A Global Review of Solid Waste Management. Urban Development Series Knowledge Papers 15. World Bank, Washington DC.
- Huet, J., Druilhe, C., Trémier, A., Benoist, J.C., Debenest, G., 2012. The Impact of compaction, moisture content, particle size and type of bulking agent on initial physical properties of sludge-bulking agent mixtures before composting. *Bioresour. Technol.* 114 (June), 428–436. <https://doi.org/10.1016/j.biortech.2012.03.031>.
- Jagadabhi, P.S., Kaparaju, P., Rintala, J., 2011. Two-stage anaerobic digestion of tomato, cucumber, common reed and grass silage in leach-bed reactors and upflow anaerobic sludge blanket reactors. *Bioresour. Technol.* 102 (7), 4726–4733. <https://doi.org/10.1016/j.biortech.2011.01.052>.
- Jha, A.K., Li, J., Nies, L., Zhang, L., 2011. Research advances in dry anaerobic digestion process of solid organic wastes. *Afr. J. Biotechnol.* 10 (64), 14242–14253.
- Kacem, M., Salvador, S., Quintard, M., 2009. Textural characterization of media composed of compacted pieces of cardboard and polyethylene using a gas tracer method. *Waste Manage.* 29 (2), 660–667. <https://doi.org/10.1016/j.wasman.2008.09.002>.
- Larsson, M.H., Jarvis, N.J., 1999. Evaluation of a dual-porosity model to predict field-scale solute transport in a macroporous soil. *J. Hydrol.* 215 (1), 153–171. [https://doi.org/10.1016/S0022-1694\(98\)00267-4](https://doi.org/10.1016/S0022-1694(98)00267-4).
- Lee, W.S., Chua, A.S.M., Yeoh, H.K., Ngoh, G.C., 2014. A review of the production and applications of waste-derived volatile fatty acids. *Chem. Eng. J.* 235 (January), 83–99. <https://doi.org/10.1016/j.cej.2013.09.002>.
- Lü, F., He, P.J., Hao, L.P., Shao, L.M., 2008. Impact of recycled effluent on the hydrolysis during anaerobic digestion of vegetable and flower waste. *Water Sci. Technol.* 58 (8), 1637–1643. <https://doi.org/10.2166/wst.2008.511>.
- Pommier, S., Chenu, D., Quintard, M., Lefebvre, X., 2007. A logistic model for the prediction of the influence of water on the solid waste methanization in landfills. *Biotechnol. Bioeng.* 97 (3), 473–482. <https://doi.org/10.1002/bit.21241>.
- Reddy, K.R., Hettiarachchi, H., Parakalla, N.n., Gangathulasi, J., Bogner, J., Lagier, T., 2009. Hydraulic conductivity of MSW in landfills. *J. Environ. Eng.* 135 (8), 677–683. [https://doi.org/10.1061/\(ASCE\)EE.1943-7870.0000031](https://doi.org/10.1061/(ASCE)EE.1943-7870.0000031).
- Richard, T.L., Veeken, A.H.M., de Wilde, V., Hamelers, H.V.M., 2004. Air-filled porosity and permeability relationships during solid-state fermentation. *Biotechnol. Prog.* 20 (5), 1372–1381. <https://doi.org/10.1021/bp0499505>.
- Rodríguez-Pimentel, R.I., Rodríguez-Pérez, S., Monroy-Hermosillo, O., Ramírez-Vives, F., 2015. Effect of organic loading rate on the performance of two-stage anaerobic digestion of the organic fraction of municipal solid waste (OFMSW). *Water Sci. Technol.* 72 (3), 384. <https://doi.org/10.2166/wst.2015.223>.
- Shewani, A. 2016. Méthanisation discontinue en voie solide statique à percolation : caractérisation et modélisation d'un système réactif à double porosité. PhD Thesis, INSA de Toulouse, Toulouse.
- Shewani, A., Horgue, P., Pommier, S., Debenest, G., Lefebvre, X., Decremps, S., Paul, E., 2017. Assessment of solute transfer between static and dynamic water during percolation through a solid leach bed in dry batch anaerobic digestion processes. *Waste Biomass Valorizat.* (July) <https://doi.org/10.1007/s12649-017-0011-1>.
- Shewani, A., Horgue, P., Pommier, S., Debenest, G., Lefebvre, X., Gandon, E., Paul, E., 2015. Assessment of percolation through a solid leach bed in dry batch anaerobic digestion processes. *Bioresour. Technol.* 178 (February), 209–216. <https://doi.org/10.1016/j.biortech.2014.10.017>.
- Sponza, D.T., Ağdağ, O.N., 2004. Impact of leachate recirculation and recirculation volume on stabilization of municipal solid wastes in simulated anaerobic bioreactors. *Process Biochem.* 39 (12), 2157–2165. <https://doi.org/10.1016/j.procbio.2003.11.012>.
- Stabnikova, O., Liu, X.-Y., Wang, J.-Y., 2008. Anaerobic digestion of food waste in a hybrid anaerobic solid-liquid system with leachate recirculation in an acidogenic reactor. *Biochem. Eng. J.* 41 (2), 198–201. <https://doi.org/10.1016/j.bej.2008.05.008>.
- Stoltz, G., Gourc, J.-P., Oxarango, L., 2010. Liquid and gas permeabilities of unsaturated municipal solid waste under compression. *J. Contam. Hydrol.* 118 (1–2), 27–42. <https://doi.org/10.1016/j.jconhyd.2010.07.008>.
- Stoltz, G., Tinet, A.-J., Staub, M., Oxarango, L., Gourc, J.-P., 2011. Moisture retention properties of municipal solid waste in relation to compression. *J. Geotech. Geoenviron. Eng.* 138 (4), 535–543.
- Tamis, J., Joosse, B.M., van Loosdrecht, M.C.M., Kleerebezem, R., 2015. High-rate volatile fatty acid (VFA) production by a granular sludge process at low PH. *Biotechnol. Bioeng.* 112 (11), 2248–2255. <https://doi.org/10.1002/bit.25640>.
- Tinet, A.-J., Oxarango, L., Bayard, R., Benbelkacem, H., Stoltz, G., Staub, M.J., Gourc, J.-P., 2011. Experimental and theoretical assessment of the multi-domain flow behaviour in a waste body during leachate infiltration. *Waste Manage.* 31 (8), 1797–1806. <https://doi.org/10.1016/j.wasman.2011.03.003>.
- Vavilin, V.A., Rytov, S.V., Lokshina, L.Y., Rintala, J.A., Lyberatos, G., 2001. Simplified hydrolysis models for the optimal design of two-stage anaerobic digestion. *Water Res.* 35 (17), 4247–4251. [https://doi.org/10.1016/S0043-1354\(01\)00148-8](https://doi.org/10.1016/S0043-1354(01)00148-8).
- Veeken, A.H.M., Hamelers, B.V.M., 2000. Effect of substrate-seed mixing and leachate recirculation on solid state digestion of biowaste. *Water Sci. Technol.* 41 (3), 255–262.
- Viéitez, E.R., Ghosh, S., 1999. Biogasification of solid wastes by two-phase anaerobic fermentation. *Biomass Bioenergy* 16 (5), 299–309. [https://doi.org/10.1016/S0961-9534\(99\)00002-1](https://doi.org/10.1016/S0961-9534(99)00002-1).
- Wu, Y.-S., 2016. Multiphase fluids in porous media. In: *Multiphase Fluid Flow in Porous and Fractured Reservoirs*. Elsevier, pp. 15–27. <https://doi.org/10.1016/B978-0-12-803848-2.00002-7>.
- Xu, S.Y., Lam, H.P., Parthiba, K.O., Wong, J.W.C., 2011. Optimization of food waste hydrolysis in leach bed coupled with methanogenic reactor: effect of PH and bulking agent. *Bioresour. Technol.* 102 (4), 3702–3708. <https://doi.org/10.1016/j.biortech.2010.11.095>.
- Yap, S.D., Astals, S., Jensen, P.D., Batstone, D.J., Tait, S., 2016. Pilot-scale testing of a leachbed for anaerobic digestion of livestock residues on-farm. *Waste Manage.* 50, 300–308. <https://doi.org/10.1016/j.wasman.2016.02.031>.